



INVESTIGATION OF FLEXURAL BEHAVIOR OF CARBON FIBER BEAMS

Mustafa Albayrak^{*1} 

¹Inönü University, Malatya OSB Vocational School, Department of Machinery and Metal Technologies, Malatya, Turkey

Abstract

Original scientific paper

In this study, beams with hat profiles were produced. For this purpose, carbon fiber woven fabrics were preferred as reinforcement elements. Afterwards, bending test was applied to these composite beams. As a result of the experiments, displacement-force graphs were obtained on the moving cylinder. In the numerical analysis section, Hashin damage criterion was preferred for damage initiation. "Continuous Damage Mechanics (CDM)" and "Material Property Degradation (MPDG)" methods are defined in the program for damage progression. In the bending test, crushing damage was observed as the dominant damage on the surface of the specimen in contact with the moving cylinder under load. Fiber breakage along with fiber tensile damage was observed on the surfaces in contact with the fixed support rollers. It was observed that the experimental results were closer to each other with the MPDG method. The convergence rate of experimental and numerical data was determined as 89.55%.

Keywords: Carbon fiber, continuum damage mechanics, hat-shape profile, material property degradation.

1 Introduction

Composite structures; It has the advantages of high specific strength, high specific stiffness and good designability. Recently, they have been widely preferred in the structural design of civil and military aircraft. Composite beams with hat-shaped profiles are one of the important structural elements that make up the main body of aircraft in the aviation industry (Figure 1). These beams have a significant impact on the strength and post-buckling bearing capacity of the hull. During use, these beams carry radial forces as well as lateral forces that cause the wing or fuselage to bend. Conducting a sound damage analysis of reinforced panels can help experts in this field design wing and fuselage integrity.

When the tests and analyzes performed on composite structures in general are examined: Li et al. (2022) experimentally performed a four-point bending test on flat profiles for numerical verification in Abaqus. Afterwards, they developed a user-defined subroutine and proposed a theoretical model. [1]. Bai et al. (2018) examined the buckling behavior and damage situations of hardened carbon fiber reinforced composite panels with I-profile under compressive load [2]. Alkhatib et al. (2020) experimentally and numerically examined the energy absorption capacity and crushing behavior of composite corrugated pipes under quasi-static axial shear crushing loading. Corrugated pipes were manufactured by wet filament winding process using Kevlar (KFRP) and carbon (CFRP) fiber reinforced composites. They carried out experimental and numerical crush tests on corrugated pipes [3]. Cherniaev et al. (2018) used the LS-DYNA

program for crush simulations of CFRPs. They performed comprehensive calibration of all material models for correlation with experiments. Three material models for this; They used MAT-54, MAT-58 and MAT-262. They reported that MAT-54 provided reasonable agreement with experimental data. They estimated the non-physical damage modes and maximum force values of MAT-58 [4]. Candido et al. (2022) established a connection between longitudinal T-profile reinforced composites and flat panels using an adhesive film layer and performed an experimental fracture analysis on the reinforced structure they obtained [5]. Dogan and Arıkan (2017) produced sandwich composites by placing PVC foam between the shell surfaces they produced from epoxy (thermosetting) and polypropylene (thermoplastic) polymer composites reinforced with E-glass. They examined the behavior of the sandwich composite panels they obtained under different impact energies [6]. Kosztowny et al. (2021) produced one-piece textile composite panels using two-dimensional and triaxial braided composites. Afterwards, they examined the buckling behavior by applying axial compression tests on the panels [7]. Kurşun et al. (2016) experimentally and numerically investigated the effect of impactor geometry on impact performance by performing low-speed impact tests on aluminum sandwich composite plates, which they produced by using a low-density polyethylene core between two aluminum plates [8]. Natarajan et al. (2023) investigated the suitability of S-Glass/carbon fiber reinforced polymer composite for submarine hull exposed to hydrostatic pressure. For this purpose, they experimentally determined the mechanical properties of S Glass/carbon fiber reinforced polymer

*Corresponding author.

E-mail address: mustafaalbayrak@inonu.edu.tr (M. Albayrak)

Received 28 March 2024; Received in revised form 30 May 2024; Accepted 07 June 2024

2587-1943 | © 2024 IJIEA. All rights reserved.

Doi: <https://doi.org/10.46460/ijiea.1460748>

composite and compared the composite with many metallic materials used in submarine hulls [9]

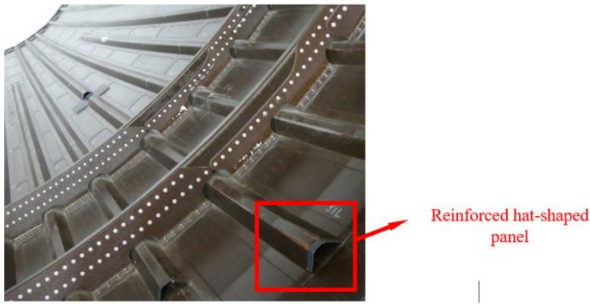


Figure 1. Reinforced hat-shaped panel in aircraft structures (Fasulo vd., 2022) [10].

When the studies in the literature are examined; When mechanical tests performed on composites with curved or flat surfaces are examined, it is seen that the focus is generally on dynamic impact tests [6,8], static pressure [3] and buckling [7] tests. A clear understanding of the damage mechanisms of structures is important in the design of flexural resistant structures.

In this study, unlike the literature, for the first time. Hat profile beams were produced by applying resin to layered carbon fiber woven fabrics under vacuum, and the mechanical behavior of the obtained specimens under bending load was examined experimentally and numerically. In the numerical part, the problem was

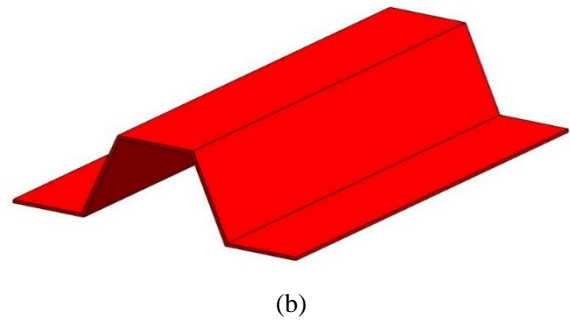
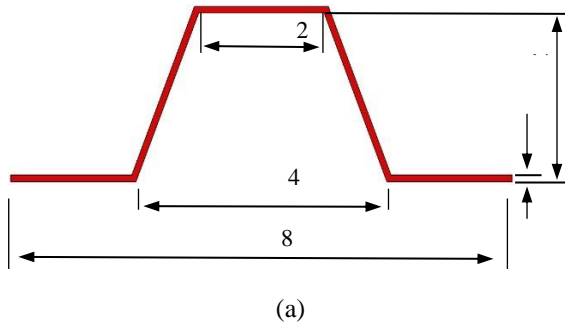


Figure 2. Hat-shaped beam a) dimensions b) solid model.

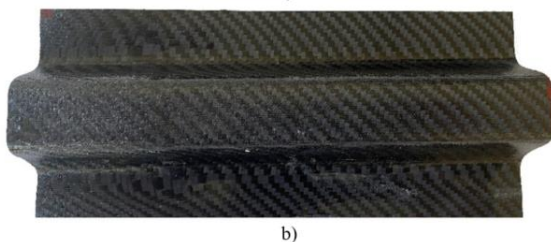
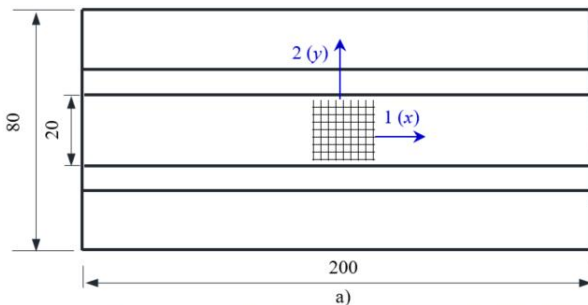


Figure 3. a) geometry dimensions of the hat-shaped profile beam. b) specimen obtained after production.

solved according to MPDG and CDM methods and the convergence to the experimental results was shown. As a result, experimental and numerical maximum contact forces are compared and presented along with force-displacement graphs.

2 Material Method

To perform bending tests on carbon fiber composite beams with a hat-shaped profile, carbon fiber composite specimens consisting of 4 layers with a thickness of 1 mm were manufactured. The profile beam dimensions are given in Figure 2. Afterwards, the beams obtained were cut in a 200 mm long wet marble cutting machine and made ready for testing. Details of the design are given in Figure 3. In this method, the mold release agent was first applied to the molds and allowed to dry. Subsequently, 245 grams per square meter of twill 2x2 woven type carbon fiber woven fabric were laid on the steel mold. Peel-ply was laid on the fabrics and adhesion was prevented with the infusion mesh that was added later. Finally, vacuum nylon was laid and the necessary tightness control was carried out. Subsequently, a mixture of MGS L160 epoxy and H160 hardener, with a weight ratio of 100:20, was impregnated on the fabrics via the vacuum infusion method. Following a 24-hour curing period, the test specimens were prepared by removing the material from the mold and cutting it into 200 mm lengths.

2.1 Three-Point Bending Test Method

Details of the ASTM D790 [11] standards test method are given in Figure 4. Here the distance between fixed supports is 180 mm

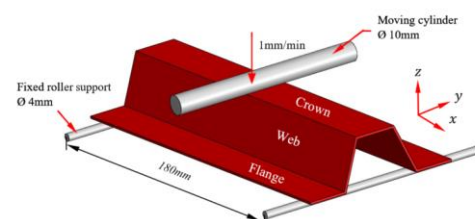
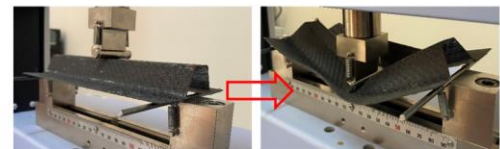


Figure 4. Test dimensions.

2.2 Numerical Analysis

In the numerical part, the analyzes were performed in Ansys Workbench 2020R1. Composite beam, moving and fixed cylinders were modeled in Solidworks program and transferred to Workbench program. 8-node element type was preferred and Multizone mesh type was used for finite element separation. Figure 5 shows the number of elements obtained after separation into finite elements of different sizes and the change in the maximum contact force accordingly. As seen in the graph, the maximum contact force remained constant after the number of elements reached 5820. Therefore, it was determined that the optimum number of elements was 5820 and the number of nodes was 33175.

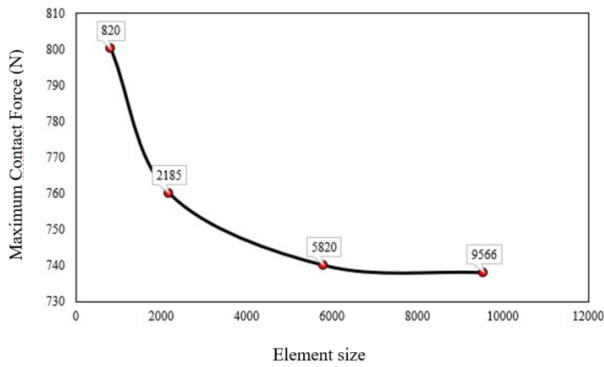


Figure 5. Mesh optimization.

2.2.1 Damage Model

In progressive damage analysis, the linear elastic orthotropic material properties of the material, the damage initiation criterion, the damage progression method, and the strength limits of the material must be defined in the program, respectively. Orthotropic material properties of carbon fiber are presented in Table 1.

Table 1. Mechanical properties of carbon fiber reinforced composite [12].

Symbol	Properties	Value	Unit
ρ	Density	1500	kg/m ³
E_x, E_y	Elasticity modulus x and y direction	43.7	GPa
E_z	Elasticity modulus z direction	14.57	GPa
ν	Poisson's ratio	0.21	-
G_{xy}	Shear modulus in xy plane	14.18	GPa
G_{yz}	Shear modulus in yz plane	14.65	GPa
G_{zx}	Shear modulus in zx plane	14.65	GPa

In order to define the beginning of damage in progressive damage analysis, Hashin damage initiation criteria must be entered into the program. The hash initiation criteria include the following four damage initiation modes. Here the damage initiation indices are I_f^t ; I_f^c ; I_m^t and I_m^c represent fiber tensile, fiber compression, matrix tensile and matrix compression damage, respectively. When any of these indices exceeds 1, damage onset occurs. Four different damage cases belonging to the Hashin criteria are evaluated according to the following formulas in Equations (1)-(4).

Fiber failure for tension ($\sigma_{xx} \geq 0$):

$$I_f^t = \left(\frac{\sigma_{xx}}{F_{xt}}\right)^2 + \alpha \left(\frac{\sigma_{xy}}{F_6}\right)^2 \tag{1}$$

Fiber failure for compression ($\sigma_{xx} < 0$):

$$I_f^c = \left(\frac{\sigma_{xx}}{F_{xc}}\right)^2 \tag{2}$$

Matrix failure for tension ($\sigma_{yy} \geq 0$):

$$I_m^t = \left(\frac{\sigma_{yy}}{F_{yt}}\right)^2 + \left(\frac{\sigma_{xy}}{F_6}\right)^2 \tag{3}$$

Matrix failure for compression ($\sigma_{yy} < 0$):

$$I_m^c = \left(\frac{\sigma_{yy}}{2F_4}\right)^2 + \left[\left(\frac{F_{yc}}{2F_4}\right)^2 - 1\right] \frac{\sigma_{yy}}{F_{yc}} + \left(\frac{\sigma_{xy}}{F_6}\right)^2 \tag{4}$$

Here σ_{ij} are the components of the stress tensor; F_{xt} and F_{xc} are the tensile and compressive strengths of a sheet in the longitudinal (fiber) direction; F_{yt} and F_{yc} are the tensile and compressive strengths in the transverse direction; F_6 and F_4 are in-plane and inter-layer shear strengths. α is the contribution of the in-plane shear stress according to this criterion and is taken as 0 in this study. In order to evaluate the damage initiation criteria in the composite structure, it is necessary to define the maximum stresses or strains that the material can tolerate before damage occurs. Stress limit values are presented in Table 2.

Table 2. Orthotropic stress limit values of carbon fiber composite [12].

Symbol	Properties	Value	Unit
X_T	Tensile strength in X direction	859	MPa
Y_T	Tensile strength in Y direction	859	MPa
Z_T	Tensile strength in Z direction	859	MPa
X_C	Compression strength in X direction	109.6	MPa
Y_C	Compression strength in Y direction	109.6	MPa
Z_C	Compression strength in Z direction	373.5	MPa
S_{XY}	Shear strength in plane $X - Y$	108.2	MPa
S_{YZ}	Shear strength in plane $Y - Z$	105.5	MPa
S_{XZ}	Shear strength in plane $X - Z$	105.5	MPa

2.2.2 Damage Evolution

MPDG and CDM methods were used for damage progression. In the MPDG method, when the breaking stress and strain are reached for the fiber and matrix components, the rate of decrease in hardness is determined separately for both components. In the CDM method, the material stiffness is gradually reduced. The stiffness reductions used for the four damage cases in the study are given in Table 3.

Table 3. Stiffness reduction coefficients for the MPDG method.

Properties	Value
Tensile fiber stiffness reduction	0.46
Compressive fiber stiffness reduction	0.46
Tensile Matrix Stiffness Reduction	0.4
Compressive Matrix Stiffness Reduction	0.4

3 Results and Discussion

Three-point bending tests were performed on specimens with hat-shaped profiles made of carbon fiber reinforced composites. In the numerical analysis section, the problem was solved and evaluated according to both Continuous Damage Mechanics (CDM) and Material Property Degradation (MPDG) methods. In both methods, the proximity of the composite structure to the damage behavior and its effect on the damage load were determined. Figure 6 shows the load-displacement curve of the specimen. The test process consists of five stages: In the first stage, the moving cylinder contacted the specimen and accordingly the reaction force values increased. At this point, elastic deformation occurred in the specimen. It was observed that the load did not increase linearly at this stage. This situation is caused by production errors and geometric discontinuities on the upper surface of the hat-shaped profile. II. With the small deformation that occurred in the specimen at this stage, the slope of the graph started to decrease further and reached the maximum damage force. Afterwards, it was observed that as the load was increased, matrix cracks spread in the structure and as a result, delamination damage occurred.

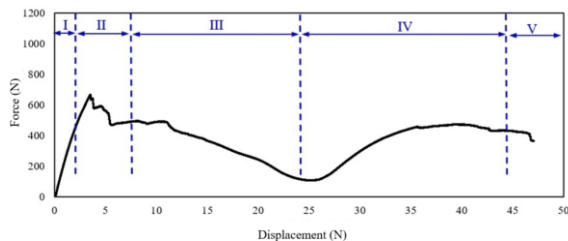


Figure 6. Force-displacement graph.

The reflection of this situation on the graph is that there are sudden and gradual decreases in load after the maximum load. III. At this stage, it was observed that the connection plates of the specimen started to open by moving in the "y" direction. Therefore, the angles made with the top surface of the connection plates that will resist the load have increased and their resistance has decreased. As a result, the load continued to decrease in an inclined manner. IV. In this stage, the moving cylinder is surrounded by the top surface of the beam with partially collapsed connecting plates. By compressing these surfaces with the cylinder that continued to move, the load-displacement curve increased slightly and then made it move horizontally. In the last stage, the moving cylinder reached its maximum displacement value. Large tensile damages were observed on the surface of the specimen below the top area, and with the progression of the damage, they turned into permanent fiber breaks. Figure 7 shows the force-displacement graph of the specimen. When the experimental graph is examined, it is evaluated that the carbon fiber beam exhibits non-linear material

behavior. However, it was observed that the slope of the force-displacement curve decreased after the experimental yield point. In the analysis section, MPDG and CDM methods were preferred for Hashin damage initiation criterion and subsequent damage progression. Obtained experimental results were compared with analysis solutions.

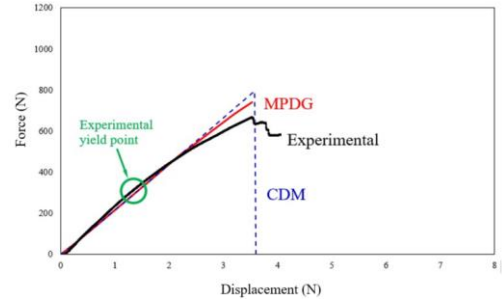


Figure 7. Experimental and numerical comparison of load-displacement graph.

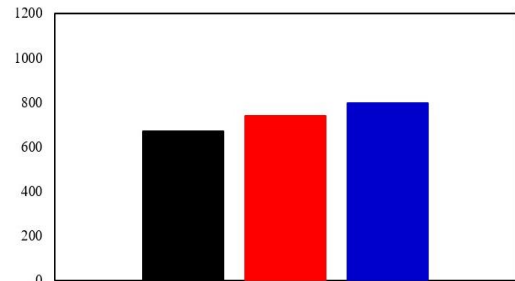


Figure 8. Experimental and numerical comparison of maximum load values.

According to the CDM method, material stiffness is gradually reduced and progress ends when catastrophic damage is reached [13]. According to the graph, it can be seen that the numerical data and experimental results are close in the elastic region. According to the CDM method, the sample suffered ultimate damage at a load of 790 N and was displaced by approximately 3.55 mm in case of ultimate damage. When the solution made with the MPDG method was examined, it was seen that the material hardness was gradually reduced. It has been observed that as the amount of displacement increases, especially in the plastic region after the yield limit, the slope begins to decrease and exhibits a behavior closer to the experimental graph. Therefore, this method comes to the fore in finite element analyzes. Zachariah.S.A., et al. They carried out experimental testing and numerical verification to investigate the in-plane tensile properties of carbon/aramid hybrid polymer composite. In their analysis with the MPDG method, they found that the composite material showed binaristic behavior and provided a slope closer to the experimental results [14]. Maximum contact forces are evaluated in Figure 8. The maximum contact force value obtained experimentally was determined as 670 N. In the MPDG and CDM methods, these values are 740N and 794N, respectively. When the convergence rates of experimental and numerical data are compared, a convergence rate of 89.55% was obtained in the solution with the MPDG method and approximately 81.49% in the solution with the CDM method.

4 Conclusion

Carbon fiber composite beams with hat-shaped profiles were produced. Three-point bending was performed on the obtained specimens. The results were compared and summarized as follows.

- The convergence rate of the MPDG method selected for damage progression to experimental results was determined to be approximately 89.55%. In the CDM method, this rate was determined as 81.49%.
- It has been determined that the MPDG method is much better than CDM. It was observed that the force-displacement graphs exhibited close behavior, especially when compared to the experimental results.
- Compression and crushing damage were seen more clearly, especially on the crown surface of the specimens. On the lower surface, mainly fiber shrinkage and fiber breakage damages were observed.
- It has been concluded that numerical modeling of composites with hat-shaped profiles, which are relatively difficult to produce experimentally, without the need for production, and solving them with the MPDG method by selecting the Hashin initial damage criterion, can give designers an idea about the mechanical behavior of composites under bending load.

Declaration

Ethics committee approval is not required.

References

- [1] Li, B., Gong, Y., Gao, Y., Hou, M., & Li, L. (2022). Failure analysis of hat-stringer-stiffened aircraft composite panels under four-point bending loading. *Materials*, 15(7), 2430.
- [2] Bai, R., Bao, S., Lei, Z., Liu, C., Chen, Y., Liu, D., & Yan, C. (2018). Experimental study on compressive behavior of I-stiffened CFRP panel using fringe projection profilometry. *Ocean Engineering*, 160, 382-388.
- [3] Alkhatib, F., Mahdi, E., & Dean, A. (2020). Crushing response of CFRP and KFRP composite corrugated tubes to quasi-static slipping axial loading: experimental investigation and numerical simulation. *Composite Structures*, 246, 112370.
- [4] Cherniaev, A., Butcher, C., & Montesano, J. (2018). Predicting the axial crush response of CFRP tubes using three damage-based constitutive models. *Thin-Walled Structures*, 129, 349-364.
- [5] Candido, G. M., Sales, R. D. C. M., Arbelo, M. A., & Donadon, M. V. (2022). Failure analysis in secondary bonded T-stiffened composite panels subject to cyclic and quasi-static compression loading. *International Journal of Adhesion and Adhesives*, 118, 103199.
- [6] Dogan, A., & Arikan, V. (2017). Low-velocity impact response of E-glass reinforced thermoset and thermoplastic based sandwich composites. *Composites Part B: Engineering*, 127, 63-69.
- [7] Kosztowny, C. J., & Waas, A. M. (2021). Postbuckling response of unitized stiffened textile composite panels: Experiments. *International Journal of Non-Linear Mechanics*, 137, 103814.
- [8] Kurşun, A., Şenel, M., Enginsoy, H. M., & Bayraktar, E. (2016). Effect of impactor shapes on the low velocity impact damage of sandwich composite plate: Experimental study and modelling. *Composites Part B: Engineering*, 86, 143-151.
- [9] Natarajan, E., Freitas, L. I., Santhosh, M. S., Markandan, K., Al-Talib, A. A. M., & Hassan, C. S. (2023). Experimental and numerical analysis on suitability of S-Glass-Carbon fiber reinforced polymer composites for submarine hull. *Defence Technology*, 19, 1-11.
- [10] Fasulo, G., Vitiello, P., Federico, L., & Citarella, R. (2022). Vibro-Acoustic Modelling of Aeronautical Panels Reinforced by Unconventional Stiffeners. *Aerospace*, 9(6), 327.
- [11] A. E883-02 (2003). Standard Guide for iTeh Standards iTeh Standards Document Preview, vol. 03, pp. 1-6.
- [12] Albayrak, M., Kaman, M. O., & Bozkurt, I. (2023). Experimental and numerical investigation of the geometrical effect on low velocity impact behavior for curved composites with a rubber interlayer. *Applied Composite Materials*, 30(2), 507-538.
- [13] Apruzzese, P., & Falzon, B. G. (2007, July). Numerical analysis of complex failure mechanisms in composite panels. In *16th international conference on composite materials, Kyoto, Japan* (pp. 234-246).
- [14] Zachariah, S. A., Shenoy, B. S., & Pai, K. D. (2021). Comprehensive analysis of in-plane tensile characteristics of thin carbon/aramid hybrid composites using experimental and RVE-based numerical study. *Composite Structures*, 271, 114160.